Multiobjective Optimization of Composite Materials for Continuous Fiber Orientation

Pedro Bührer Santana[1,2], Marcos Daniel de Freitas Awruch[1,2], Ewerton Grotti[1], and Herbert Martins Gomes[1(✉)]

[1] Federal University of Rio Grande do Sul, Porto Alegre, Brazil
pedrobs66@gmail.com, marcos.dfa@gmail.com,
ewerton.grotti@ufrgs.br, herbert@mecanica.ufrgs.br
[2] Federal University of Santa Maria, Santa Maria, Brazil

Abstract. Composite materials have gained prominence as an intensively used material in the aerospace and mechanical industry due to their characteristics of stiffness and low weight. The possibility of designing composite specimens with continuous orientation of the fibers at the ply level, following smooth contours, makes this material even more attractive, as it assess, in a more rational way, the whole reserve of fiber stiffness in the directions of main loadings. This work presents a methodology for the optimization of composite materials by the definition of a continuous fiber orientation. Parameterized curves are used to define the continuous orientation of the fibers and the control points are assumed as design parameters during optimization. A Multiobjective Quantum Particle Swarm Optimization (MO-QPSO) algorithm is used as an optimizer due to desirable characteristics of good convergence and lower likelihood of being stuck in local minima. Two examples are presented; both have as one of the objective functions the Practicality Index (a value that defines the ease of execution of the continuous orientations of the fibers). The first one is a dynamic analysis where the previous objective is confronted with the maximization of the first natural frequency. The next example is a trade-off with the Tsai-Wu failure criteria and the Practicality Index. The results are compared with literature solutions (which uses an improved NSGA-II algorithm). In the end, the orientation of the fibers found in the composite material was very similar to those reported in the literature, confirming the validity of the proposed methodology.

Keywords: Multiobjective optimization · Composite material
QPSO · Continuous fiber orientation

1 Introduction

Composite materials optimization is a trending topic in industry and academic research, where the maximum performance commonly is the main objective for each application. Usually, the available parameters for the project tuning are the number of plies, stack sequence, a fixed fiber orientation per ply, and proprieties of fiber and matrix constituents. Depending on the fabrication process, not all options and even some uncertainties might be present. There are developments in that area to keep the project under high standards and also providing new products configurations, such as

continuous fiber orientation variation in the same ply. That is a new opportunity for the development of highly efficient structures, where the static or dynamic behavior might reach optimal efficiency.

This work aims the optimization of composite materials for continuous fiber orientation, a recent and ongoing capability in new fabrication processes. It is presented two examples for static and dynamic analysis, the first one taking into account the Tsai-Wu index and the Practicality index (a value considering the fiber steering curvature, representing its fabrication feasibility). The second example first two natural frequencies of a composite plate are related, where the objective is its separation. The results are compared with literature ones.

2   Brief Bibliographical Review

Composite materials optimization is a recurrent theme in the academic community, since its wide applicability. Khandan et al. [1] presented a monobjective optimization using a Simulated Annealing algorithm, where fibers orientation is the design variable in a transverse shear sensitive model, where the minimization of the composite thickness is the goal. The results were compared with prototypes and presented a very good agreement with the numerical simulation.

In a similar objective of minimizing the plate thickness, Rettenwander et al. [2] developed a hybrid algorithm where the fiber orientation is determined locally based on the principal stresses. The results present a continuous fiber orientation through a numerical example.

A methodology called level set is presented by Lemaire et al. [3] to maximize the stiffness of composite materials for curved fiber trajectories. The fiber orientation free of the stacking sequence, avoiding overlaps and voids between successive layers is the main advantage.

Honda et al. [4] proposed a multiobjective optimization through continuous curvilinear composite plates tailoring using a NSGA-II algorithm. Three numerical examples were presented in the paper. Two aimed at maximizing the first natural frequency and minimizing the sum of the curvature of the fibers (practicality index) in different boundary conditions. The third one aimed at minimizing both the Tsai-Wu index and the practicality index. These examples and results obtained by Honda et al. were taken as the basis of validation in the present work.

3   Theoretical Basis

3.1   Formulation for Laminated Orthotropic Plates

The fiber-reinforced composites are anisotropic or, often, orthotropic materials where its main stiffness and strength properties are in the longitudinal fiber direction. In the constitutive formulation, it is considered different Poisson ratios and Young's moduli for each main direction. For the applied finite element method in this paper, the orthotropic plates have null transverse stress and the cross shear stresses are assumed as

a linear variation along the width, based on the First Order Shear Deformation Theory (FSDT) model (Jones [5]). The displacement field is given by Mindlin's theory of plates by:

$$u(x, y, z) = u_0(x, y) + z\theta_x(x, y)$$
$$v(x, y, z) = v_0(x, y) + z\theta_y(x, y) \tag{1}$$
$$w(x, y, z) = w_0(x, y)$$

The stiffness matrix for each element is divided into components corresponding to effects from membrane stiffness, membrane-bending coupling, bending itself and shear, as shown below:

$$\mathbf{K} = \mathbf{K_m} + \mathbf{K_{mb}} + \mathbf{K_{bm}} + \mathbf{K_b} + \mathbf{K_s} \tag{2}$$

More detailed information on this formulation can be obtained in Ferreira [6].

With the assembled global mass and stiffness matrices, the natural frequencies and modes are the solutions of the eigenvalue equation

$$\left(\omega_i^2 \mathbf{M}^g - \mathbf{K}^g\right)\varphi_\mathbf{i} = 0 \tag{3}$$

where ω_i corresponds to the natural frequencies and $\varphi_\mathbf{i}$ the respective mode shape. In this work, the finite element is the degenerate Serendipity element of eight nodes.

3.2 Tsai-Wu Failure Criteria

The Tsai-Wu failure criterion is commonly used for composite materials in plane stress. The failure occurs when the following relationship is violated:

$$H_1\sigma_1 + H_2\sigma_2 + H_{11}\sigma_1^2 + H_{22}\sigma_2^2 + H_{66}\tau_{12}^2 + H_{12}\sigma_1\sigma_2 - 1 < 0 \tag{4}$$

or

$$\Phi < 0 \tag{5}$$

where H are strength tensors corresponding to tensile and compressive loads

$$H_i = \frac{1}{\sigma_i^t} + \frac{1}{\sigma_i^c} \quad \text{and} \quad H_{ij} = \frac{1}{\sigma_i^t\sigma_j^c} \tag{6}$$

3.3 Fiber Angles and Practicality Index

A third-degree polynomial function f with two variables is used as reference to obtain the angle of each fiber, through the tangential direction of its contour lines, taken in the central coordinates of each element.

$$f(x, y) = c_{00} + c_{10}x + c_{01}y + c_{20}x^2 + c_{11}xy + c_{02}y^2 + c_{30}x^3 + c_{21}x^2y + c_{12}xy^2 + c_{03}y^3$$

$$\tag{7}$$

$$\theta_n = tan^{-1}\left[-(f_x)/(f_y)\right] \tag{8}$$

where the subscripts refer to which variable the partial derivatives is calculated.

Depending on the boundary conditions and its symmetry, some constants of the polynomial can be null. The surface curvature at any point is defined as:

$$k(x, y) = \frac{1}{\left(f_x^2 + f_y^2\right)}\begin{bmatrix} -f_x & f_y \end{bmatrix}\begin{bmatrix} f_{xx} & f_{xy} \\ f_{xy} & f_{yy} \end{bmatrix}\begin{bmatrix} -f_y \\ f_x \end{bmatrix} \tag{9}$$

The practicality index, a value that is associated with the ease of production, since it is related with the level of fiber curvature in the plate, is calculated as the mean of k for all n_e elements:

$$\bar{k} = \sum_{i=1}^{ne} k(x, y)^i \tag{10}$$

4 Multiobjective Optimization

Many engineering design problems are multi-objective in nature because they often involve more than one goal to be optimized. These objectives impose potentially conflicting requirements such as the technical and economic performance of a given system. The designer may formulate a multi-objective optimization problem if he wants to study the trade-offs between these conflicting objectives and explore the available design options. Once there are conflicting requirements or goals, a multiobjective optimization is a suitable approach to a problem. The trade-off among the n different objectives is a decision that should be taken by the designer, chosen from a Pareto front of solutions. The solutions of that front are called non-dominated. A feasible solution X^1 dominates another solution X^2 if (for a minimization problem):

$$g_i\left(X^1\right) \leq g_i\left(X^2\right) \forall i = 1, 2, \ldots, n.$$
$$g_i\left(X^1\right) < g_i\left(X^2\right) \text{ for at least one } i \tag{11}$$

where $g_i(X)$ are the objective functions.

4.1 Quantum Particle Swarm Optimization (QPSO)

The Quantum Particle Swarm Optimization method (QPSO) was developed by Sun et al. [7] and has a better convergence behavior when compared to PSO (Yang et al. 2013). Instead of position and velocity, the state of the particles in the QPSO is updated by the square of the module of a wave function $|\psi(x,t)|^2$, that represents the

probability density of particles in a position to appear. Using Monte Carlo method, the state of the particles can be determined by Eqs. (11), (12) and (13).

$$\begin{aligned} x_{ij}(t+1) &= P_{ij} - \beta.\big(mbest_j(t) - x_{ij}(t)\big).\ln\big(1/u_{ij}(t)\big), \quad for\ \rho \geq 0.5 \\ x_{ij}(t+1) &= P_{ij} + \beta.\big(mbest_j(t) - x_{ij}(t)\big).\ln\big(1/u_{ij}(t)\big), \quad for\ \rho < 0.5 \end{aligned} \tag{12}$$

$$P_{ij}(t) = \varphi_j(t).pbest_{ij}(t) + \big(1 - \varphi_j(t)\big).gbest_{ij}(t) \tag{13}$$

$$mbest_j(t) = \frac{1}{n}\sum_{i=1}^{n} pbest_{ij}(t) \tag{14}$$

$$\beta(t) = ((\beta_1 - \beta_0)(T - t)/T) + \beta_0 \tag{15}$$

where *pbest* is the local best position of each particle, *gbest* is the global best position of the swarm, and *mbest* is the mean best position of all best positions, *pbest*, of the population. n is the size of the swarm population, t is the iteration time-step, T is the total number of iterations, and β_1 and β_0 are superior and inferior limits for the coefficient, and β is called contraction-expansion coefficient, which controls the convergence of the algorithm. ρ, u and φ are uniformly distributed random numbers between 0 and 1.

4.2 Multiobjective Quantum Particle Swarm Optimization (MOQPSO)

The method applied by the authors is based on the Pareto Front archive strategy, as described by Branke and Mostaghim [8]. The methodology consists in keeping all the best particles of the current iteration stored in a database. Those particles will guide the next generation, and a special treatment is given to the extreme particles, in the search domain, that will stimulate a spread searching effort, avoiding a short and concentrated Pareto Front. The MOQPSO considers 3 archives in objective function space: (*i*) archive f_P for storing local best positions, (*ii*) archive f_{G1} for storing global best positions and (*iii*) archive f_{G2}, for storing global best positions that are filtered by a minimum distance criteria. The corresponding set of design variables vectors corresponding to each of the archives are X_G, X_{G1} and X_{G2}.

Instead of using the classical *meanbest* variable of the QPSO, this algorithm uses guide-particles in order to direct the particles towards the Pareto Front. The guide selection is made randomly in two ways: (*i*) using one of the previously explained extreme solutions as a guide and (*ii*) using the closest solution (in Euclidean Norm sense) belonging to the Pareto Front in the current iteration.

An extreme-particle maintenance technique is applied in order to keep the boundaries as wide as possible. A criterion of proximity in the objective function space is also employed in order to avoid crowding of particles in some regions or unnecessary movements in already populated regions of search space. This algorithm was successfully tested and compared by Grotti et al. (2017) for multiobjective optimizations of mode frequencies and accelerations of vehicle suspension models, using similar algorithms such as NSGA-II.

5   Numerical Examples

5.1   Frequency Maximization on a Fully Clamped Square Plate (CCCC)

In this example, a square plate fully clamped, characterized in a mesh of 100 regular size elements is analyzed, where the objectives are the maximization of the first natural frequency while reducing the mean curvature (Practicality Index). The composite plate has 8 layers with thickness 0.125 mm, and the following properties: E_1= 138 GPa, E_2 = 8.96 GPa, G_{12}= 7.10 GPa, v_{12}= 0.3 and ρ = 1578 kg/m³. The fiber arrangement is defined in the first layer and the stack is configured as [(+layer/−layer)₂]ₛ.

The natural frequencies are normalized as indicated below:

$$\Omega = \omega a^2 \sqrt{\rho h / D_0} \tag{16}$$

where a is the plate length, h the total thickness and $D_0 = E_2 h^3 / [12(1 - v_{12} v_{21})]$.

The Pareto Front is presented in Fig. 1, where the results are compared with the ones obtained by Honda et al. [4]. Those objectives functions are conflicting since larger bends will generate higher frequency values. There are three different configurations of this optimal front indicated on Fig. 1 that has its fiber arrangement shown in Fig. 2.
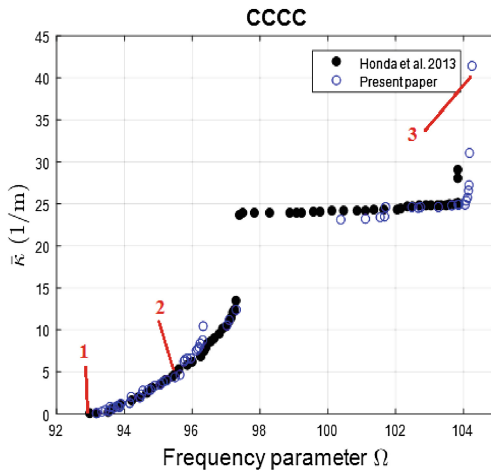
Fig. 1. Pareto Front with results obtained by Honda et al. [4] and by the present paper.

Table 1 reports the values for the dimensionless natural frequency and the mean curvature for the highlights points in the Pareto Front indicated in Fig. 1. Table 2 shows the polynomial coefficients for those cases.
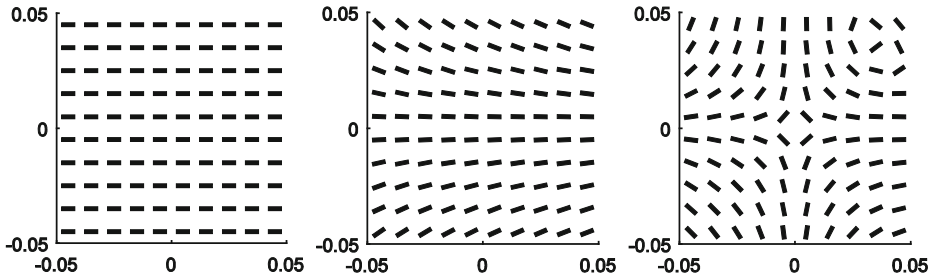
Fig. 2. From left to right, the configurations 1, 2 and 3, respectively, indicated in Fig. 1.

Table 1. Comparison between results obtained in the article and those obtained by the model proposed in the work for the CCCC case.

Case	Natural frequency [Hz]	Mean Curvature [1/m]
(1) Honda et al. [4]	93.64	$5.3 \cdot 10^{-4}$
(2) Honda et al. [4]	95.64	5.06
(3) Honda et al. [4]	103.9	29.03
(1) this work	93.19	$1.24 \cdot 10^{-4}$
(2) this work	95.64	4.73
(3) this work	104.25	41.41

Table 2. Polynomial coefficients for the CCCC case.

Pareto Solution	Polynomial Coefficients using MO-QPSO									
	c_{00}	c_{10}	c_{01}	c_{20}	c_{11}	c_{02}	c_{30}	c_{21}	c_{12}	c_{03}
(1)	1.0	0.0	2.0	0.0	0.0	-2.0	0.0	0.0	2.0	2.0
(2)	-2.0	0.0	0.1	0.0	1.0	0.0	0.0	2.0	1.0	-2.0
(3)	-0.9	0.0	0.0	0.0	-0.2	0.0	0.0	2.0	1.8	0.0

5.2   Stress Concentration on a Plate with a Center Hole

Due to the symmetry of the problem, a quarter of the structure is modeled. This plate has a width of 10 cm, 70 cm in length and a center hole of 5 cm radius. The stack sequence pattern and the composite properties are similar to the previous example. The mesh of 400 elements is shown in Fig. 3. The elongated plate is used to guarantee a valid stress state near the hole, and the results are shown in an area of 10 cm by 10 cm in the stress concentration region on the left. Since the stresses don't change with thickness, the evaluation is made only in the first two layers.

The load is applied distributed on the right end nodes, generating 10 MPa of axial tensile. The failures stress parameters are: $\sigma_1^t = \sigma_2^c = 144800$ N/cm^2, $\sigma_2^t = 5171$ N/cm^2, $\sigma_2^c = 20685$ N/cm^2 and $\tau_{12} = 9008$ N/cm^2.

The Pareto Front for this example is shown in Fig. 4, where the results from Honda et al. [4] and the present work are confronted. In Fig. 5 the first and second
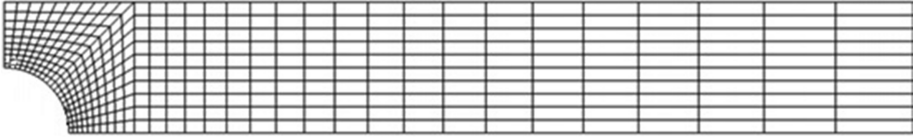
Fig. 3. Mesh generated of a quarter plate.
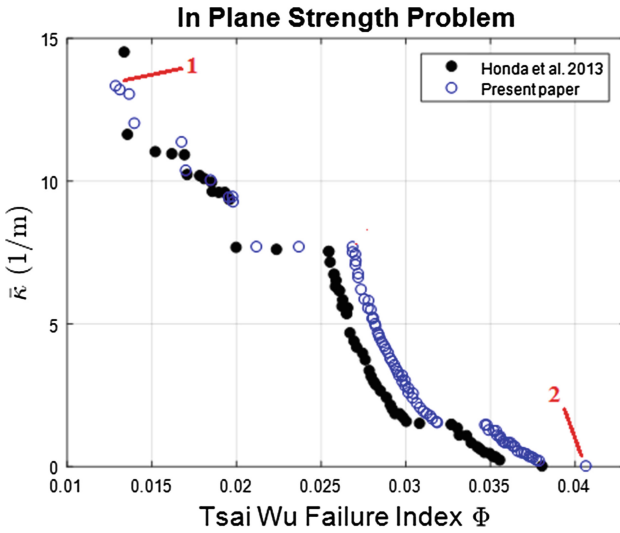
Fig. 4. Pareto Front with results obtained by Honda et al. [4] and by the present paper.
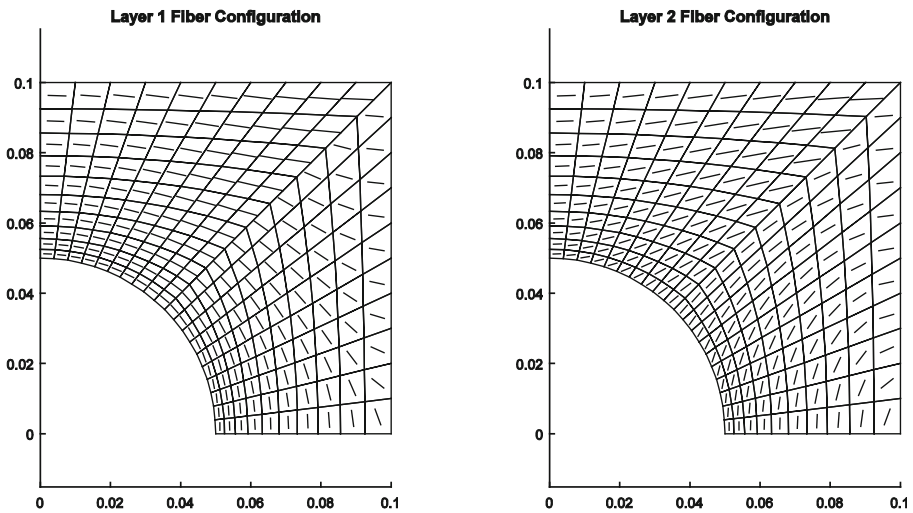
Fig. 5. Results for configuration 1 in the first (left) and second (right) layers.
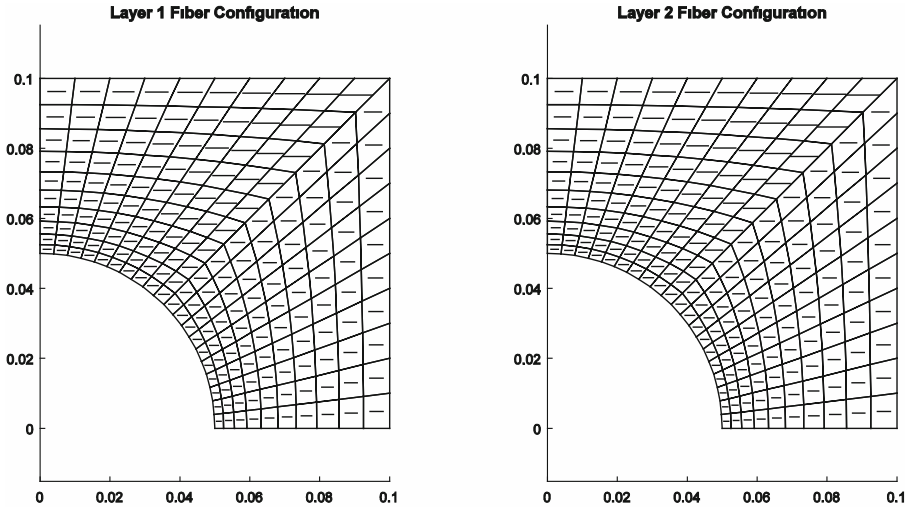
Fig. 6. Results for configuration 2 in the first (left) and second (right) layers.

layers are presented for the configuration 1 indicated in Fig. 4, while in Fig. 6, are the results for configuration 2.

6   Conclusions

The main objective of this work was the validation of the continuous fiber orientation in plate models optimized with a MO-QPSO algorithm, tested in dynamic and static conditions, confronted with a fabrication process index (practicality index). The examples were selected to match literature results, mainly by Honda et al. [4]. In the first example, the MO-QPSO was able to spread the Pareto Front, finding and extreme configuration (number 3). But it lacked performance to populate the middle region of the front. For the second example, the right side of the front presented an offset that is subject of an ongoing investigation. In spite of that, the results of fiber orientation are similar from that presented in the literature. The grown interest in multiobjective optimization and in continuous fiber orientation is a strong incentive of research in that subject.

References

1. Khandan, R., Noroozi, S., Sewell, P., Vinney, J., Koohgilani, M.: Optimum design of fibre orientation in composite laminate plates for out-plane stresses. Adv. Mater. Sci. Eng. 11 (2012)
2. Rettenwander, T., Fischlschweiger, M., Steinbichler, G.: Computational structural tailoring of continuous fiber reinforced polymer matrix composites by hybridization of principal stress and thickness optimization. Compos. Struct. **108** (2014)

3. Lemaire, E., Zein, S., Bruyneel, M.: Optimization of composite structures with curved fiber trajectories. Compos. Struct. **131** (2015)
4. Honda, S., Igarashi, T., Narita, Y.: Multi-objective optimization of curvilinear fiber shapes for laminated composite plates using NSGA-II. Compos. Part B Eng. **45**(1) (2013)
5. Jones, R.M.: Mechanics of Composite Materials, 2nd edn. Taylor & Francis Group, New York (1999)
6. Ferreira, A.J.M.: MATLAB Codes for Finite Element Analysis. Springer, Netherlands (2009)
7. Sun, J., Feng, B., Xu, W.: Particle swarm optimization with particles having quantum behavior. In: Proceedings of Congress on Evolutionary Computation, Portland, OR, USA (2004)
8. Branke, J., Mostaghim, S.: About selecting the personal best in multiobjective particle swarm optimization. In: Parallel Problem Solving from Nature-PPSN IX, 4196 (2006)
9. Grotti, E., Awruch, M.D.F., Gomes, H.M. Otimização Multiobjetivo de Parâmetros de Suspensão Veicular com algoritmo QPSO. In: Proceedings of DINCON 2017, Braizilian Conference in Dynamics, Control and Applications, São José do Rio Preto, São Paulo (2017)